



V/f SPEED CONTROL OF FIVE-PHASE PERMANENT MAGNET SYNCHRONOUS MOTOR FED BY INDIRECT MATRIX CONVERTER WITH CARRIER-BASED PWM

Dr. Turki Khawish Hassan¹, *Zainab Mahmood Abed²

- 1) Assistant Prof., Electrical Engineering Department, University of Mustansiriyah, Baghdad, Iraq.
- 2) M.Sc. student, Electrical Engineering Department, University of Mustansiriyah University, Baghdad, Iraq.

Abstract: This paper presents the V/f method to control the speed of five phase Permanent Magnet Synchronous Motor (PMSM). The Indirect Matrix Converter (IMC) is used to supply the five-phase PMSM from three-phase AC voltages source. The carrier-based PWM (CBPWM) based on space vector modulation analysis is used to control the IMC with a fixed slope carrier signal, it is used to provide a sinusoidal output current by neglecting the d_3 - q_3 currents. Five-phase PMSM is used due to its advantages over traditional three-phase PMSM. The simulation is executed using MATLAB/Simulink environment, different cases are applied by change the load and speed of the motor to study the performance of the system.

Keywords: Indirect Matrix Converter, Space Vector PWM, five-phase Permanent Magnet Synchronous Motor, V/f speed control

السيطرة على سرعة محرك مغناطيسي تزامني خماسي الطور بطريقة V/f يغذيه محول المصفوفة الغير مباشر باستخدام معدل عرض النبضة المعتمد على الناقل

الخلاصة: هذا البحث يوضح استخدام طريقة V/f للسيطرة على سرعة محرك ذو مغناطيس دائم تزامني خماسي الطور، تم استخدام محول المصفوفة الغير مباشر لتجهيز المحرك من مصدر فولتية متناوب ثلاثي الطور، تم استخدام معدل عرض النبضة المعتمد على الناقل بالاعتماد على تحليل معدل متجهات الفراغ للسيطرة على المحول باستخدام ناقل ذو ميل ثابت لتجهيز تيار خرج جيبي عن طريق الغاء تيارات d_3 - q_3 . استخدم المحرك خماسي الطور لمزاياه مقارنة مع المحرك ثلاثي الطور التقليدي. تم تنفيذ المحاكاة باستخدام MATLAB/Simulink، تم تطبيق حالات مختلفة بتغيير الحمل و السرعة لدراسة اداء المنظومة.

1. Introduction

The IMC is one of the most interesting families of the converters, its construction based on the AC/DC/AC voltage conversion, so it is divided into two stages; rectifier stage and inverter stage. It is fed directly from 3-phase AC voltage supply (Grid) to three or multi-phase load, without use large passive components to store the energy. The most advantages of the IMC are sinusoidal input and output current waveforms, unity power factor, and ability of four-quadrant operation [1].

*Corresponding Author zainab.mahmood21290@gmail.com

The authors in [2] proposed the carrier-based PWM (CBPWM) method to control the switches of IMC where the IMC is implemented to feed three-phase RL-load by using DSP and Complex Programmable Logic Device (CPLD). The method is also used in [1] to feed dual three-phase RL-loads by a single three-phase power supply and enhance the maximum IMC voltage transfer ratio. In [3] the CBPWM method is used to reduce the IMC switching losses by avoiding the switching at output current peak value. In [4] the CBPWM is used for three-to-five IMC to feed five-phase RL-load by three-phase power.

The PMSM has high performance with high residual flux and coercively over other types of AC motors [5], The multi-phase drives have other advantages over traditional three-phase drives such as reducing the power requirement for the semiconductor devices of the converter and higher load power can be obtained due to dividing the required power between multi-phases [6].

By applying the V/f method, it is possible to adjust the motor speed by control the frequency and the stator voltage amplitude, the ratio of the voltage amplitude to frequency (V/f) should be kept constant. This method is characterized by its simplicity, easy to implement, independently of the drive parameters, and low cost. The stator resistance must be taken into account as its voltage drop must be compensated at low frequency operation by boosting the stator voltage [7].

The CBPWM method is not used to control the IMC switches with five-phase PMSM up to this time, it is only used with RL-load. The novelty of this paper is to use the open loop V/f approach to control the speed of the five-phase PMSM using three-phase to five-phase IMC. The CBPWM method is used to control the switching of the IMC, it is based on space vector PWM (SVPWM) with symmetrical triangular carrier signal [4]. By applying the CBPWM method the two stages of the IMC are coupled physically and the load voltages are specified by 3-phase AC supply voltages and switching functions [8].

2. The Indirect Matrix Converter

The IMC is consisted of rectifier and inverter stages as shown in figure (1) [1]. The rectifier stage converts voltages from the grid (3-phase AC voltages) to DC voltage, which fed immediately to the inverter stage through three branches of two bidirectional switches. The inverter stage converts that DC voltage to five-phase AC voltages, with variable amplitude and frequency, through five branches of two unidirectional switches. The clamp circuit, which contents a simple diode in series with small size capacitor, is used to absorb the magnetic energy stored in the input filter inductors when a fault occur causing turn off the converter [8].

The space vector analysis of the IMC based on the analysis of the reference input current space vectors of the rectifier stage, and the reference output voltage space vectors of the inverter stage [2], are demonstrated in the following subsections:

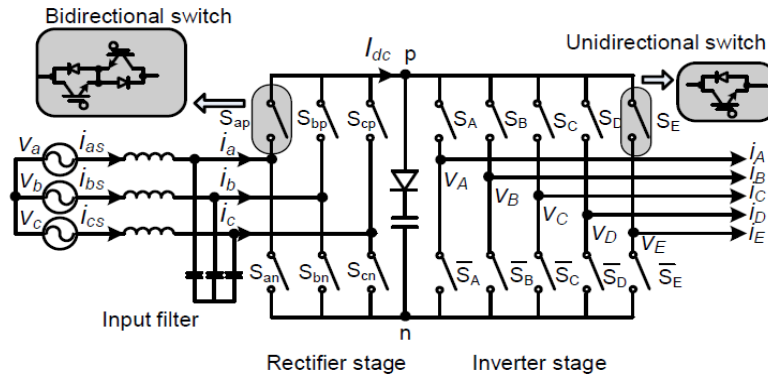


Figure (1): Three to five phase IMC construction

2.1. Rectifier Stage

The three phase grid voltages are balanced, so the input phase voltages have two conditions to separate six sectors. First condition, one positive input phase voltage and two are negative (sectors 1,3,5). Second condition, two positive input phase voltages and one is negative (sectors 2,4,6) [2] as shown in figure (2). It is assumed that the three-phase grid voltage are given as:

$$v_a = V_{in} \cos(\omega_{in}t) \tag{1}$$

$$v_b = V_{in} \cos(\omega_{in}t - 2\pi/3) \tag{2}$$

$$v_c = V_{in} \cos(\omega_{in}t + 2\pi/3) \tag{3}$$

where; V_{in} and ω_{in} represent the amplitude and angular frequency of the input phase voltage.

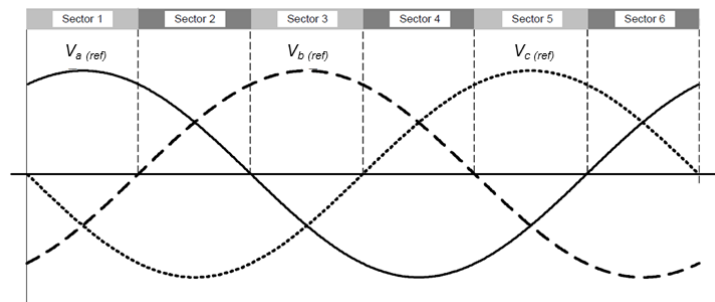


Figure (2): Three-phase input voltage divided into six sectors

Table (I) shows the six possible active switching states and the input current space vectors, where I_{dc} represents the dc-link current. It is clear from the table that the current vectors have six fixed direction, as shown in figure (3-a).

There are two adjacent active current vectors chosen to generate the reference input current vector depending on its position, as example the reference input current vector with θ_{in} between $-\pi/6$ and $\pi/6$ laying in sector 1, it is generated by two vectors I_{ab} and

I_{ac} , where these two vectors represent the connection of positive pole of input phase a to the negative poles of input phases b and c , as shown in figure (3-b).

Table (I): switching states and the input current space vectors of rectifier stage

Switching State						Input Current	
S_{ap}	S_{bp}	S_{cp}	S_{an}	S_{bn}	S_{cn}	Magnitude	Phase
1	0	0	0	1	0	$2/\sqrt{3} I_{dc}$	$-\pi/6$
1	0	0	0	0	1	$2/\sqrt{3} I_{dc}$	$\pi/6$
0	1	0	0	0	1	$2/\sqrt{3} I_{dc}$	$\pi/2$
0	1	0	1	0	0	$2/\sqrt{3} I_{dc}$	$5\pi/6$
0	0	1	1	0	0	$2/\sqrt{3} I_{dc}$	$7\pi/6$
0	0	1	0	1	0	$2/\sqrt{3} I_{dc}$	$3\pi/2$

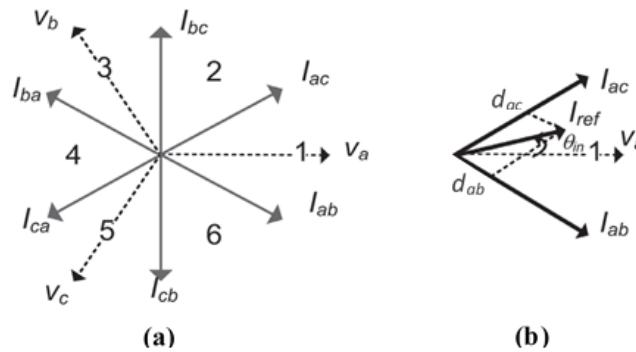


Figure (3): The space vector diagram of the rectifier stage

The duty cycles of the two active vectors of sector 1, I_{ab} and I_{ac} , are given as d_{ab} and d_{ac} :

$$d_{ab} = m_r \sin (\pi/6 - \theta_{in}) \tag{4}$$

$$d_{ac} = m_r \sin (\theta_{in} + \pi/6) \tag{5}$$

and the other one is the duty cycle of the zero vector, which mean there is no input voltage applied to dc-link voltage.

$$d_0 = 1 - d_{ab} - d_{ac} \tag{6}$$

where; m_r is the modulation index of the rectifier stage, θ_{in} is the angle of the reference input current vector

In order to obtain the maximum dc-link voltage, the zero vectors are not considered. Hence, the switching sequence consists only the two active current vectors I_{ab} and I_{ac} , and their duty cycles are recalculated and defined as d_x and d_y , respectively:

$$d_x = \frac{d_{ab}}{d_{ab}+d_{ac}} = -\frac{\cos(\theta_{in}-\frac{2\pi}{3})}{\cos(\theta_{in})} = -\frac{v_b}{v_a} \tag{7}$$

$$d_y = \frac{d_{ac}}{d_{ab}+d_{ac}} = -\frac{\cos(\theta_{in}+\frac{2\pi}{3})}{\cos(\theta_{in})} = -\frac{v_c}{v_a} \tag{8}$$

According to above equations the average value of dc-link voltage per one sampling period is:

$$\bar{V}_{dc} = d_x v_{ab} + d_y v_{ac} = 3 \frac{V_{in}^2}{2v_a} \tag{9}$$

Figure (4) shows the dc-link voltage and its average value which generated by the rectifier stage control, the \bar{V}_{dc} varies by six times the frequency of the input voltage, the respective maximum and minimum values of the average \bar{V}_{dc} are:

$$\bar{V}_{dc(max)} = \sqrt{3} V_{in} \tag{10}$$

$$\bar{V}_{dc(min)} = \frac{3V_{in}}{2} \tag{11}$$

Applying the same approach, the other sectors duty cycles and switching states can be obtained, and all these information states in table (II).

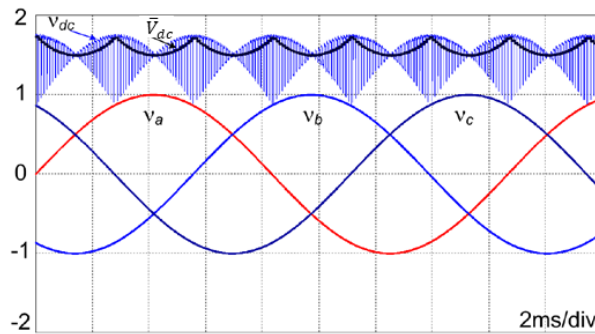


Figure (4): The dc-link voltage (v_{dc}) and its average value (\bar{V}_{dc})

Table (II): Switching states and duty cycles of the active vectors and dc-link average voltages for rectifier stage

Input voltage phase $\omega_{in}t$	Sector	ON switch	Modulated switches and duty cycles				Average dc-link voltage (\bar{V}_{dc})
			d_x		d_y		
$-\pi/6 \dots \pi/6$	1	S_{ap}	S_{bn}	$-v_b/v_a$	S_{cn}	$-v_c/v_a$	$3V_{in}^2/2v_a$
$\pi/6 \dots \pi/2$	2	S_{cn}	S_{bp}	$-v_b/v_c$	S_{ap}	$-v_a/v_c$	$-3V_{in}^2/2v_c$
$\pi/2 \dots 5\pi/6$	3	S_{bp}	S_{cn}	$-v_c/v_b$	S_{an}	$-v_a/v_b$	$3V_{in}^2/2v_b$
$5\pi/6 \dots 7\pi/6$	4	S_{an}	S_{cp}	$-v_c/v_a$	S_{bp}	$-v_b/v_a$	$-3V_{in}^2/2v_a$
$7\pi/6 \dots 9\pi/6$	5	S_{cp}	S_{an}	$-v_a/v_c$	S_{bn}	$-v_b/v_c$	$3V_{in}^2/2v_c$
$9\pi/6 \dots 11\pi/6$	6	S_{bn}	S_{ap}	$-v_a/v_b$	S_{cp}	$-v_c/v_b$	$-3V_{in}^2/2v_b$

2.2. Inverter Stage

The desired five-phase output voltage is symmetrical and displaced by $2\pi/5$, as follow:

$$v_A = V_{out} \cos(\omega_{out}t) \quad (12)$$

$$v_B = V_{out} \cos(\omega_{out}t - 2\pi/5) \quad (13)$$

$$v_C = V_{out} \cos(\omega_{out}t - 4\pi/5) \quad (14)$$

$$v_D = V_{out} \cos(\omega_{out}t - 6\pi/5) \quad (15)$$

$$v_E = V_{out} \cos(\omega_{out}t - 8\pi/5) \quad (16)$$

where; V_{out} and ω_{out} represent the amplitude and angular frequency of the output phase voltage.

The five-phase system can be decomposed in the form of four symmetrical system with a zero sequence vector (homopolar):

$$[M_5] = \begin{bmatrix} 1 & 1 & 1 & 1 & 1 \\ 1 & a & a^2 & a^3 & a^4 \\ 1 & a^2 & a^4 & a & a^3 \\ 1 & a^3 & a & a^4 & a^2 \\ 1 & a^4 & a^3 & a^2 & a \end{bmatrix} \quad (17)$$

where; $a = e^{2\pi/5}$

In the above system, all vectors are orthogonal, it can be defined three orthogonal subspaces: first subspace is the main frame which deduced from 2nd and 5th columns, second subspace is the auxiliary frame which deduced from 3rd and 4th columns, and last one is the zero sequence which deduced from the 1st column. The harmonics distribution of five-phase system is states in table (III).

Table (III): Harmonic distribution of five-phase system

Subspaces	Main frame	Auxiliary frame	Homopolar
Harmonic order	1, 4, 6, 9, ...	3, 2, 7, 8, ...	5, 10, 15, ...

It is clear that the positive sequence of the main frame indexed on the fundamental, and on the third harmonic for the auxiliary frame, so the space vector of the output voltage is defined as [5]:

$$\begin{bmatrix} V_{d1} \\ V_{q1} \\ V_{d3} \\ V_{q3} \\ 0 \end{bmatrix} = \sqrt{\frac{2}{5}} \begin{bmatrix} 1 & \cos \alpha & \cos 2\alpha & \cos 3\alpha & \cos 4\alpha \\ 0 & \sin \alpha & \sin 2\alpha & \sin 3\alpha & \sin 4\alpha \\ 1 & \cos 3\alpha & \cos 6\alpha & \cos 9\alpha & \cos 12\alpha \\ 0 & \sin 3\alpha & \sin 6\alpha & \sin 9\alpha & \sin 12\alpha \\ \frac{1}{\sqrt{2}} & \frac{1}{\sqrt{2}} & \frac{1}{\sqrt{2}} & \frac{1}{\sqrt{2}} & \frac{1}{\sqrt{2}} \end{bmatrix} \begin{bmatrix} V_A \\ V_B \\ V_C \\ V_D \\ V_E \end{bmatrix} \quad (18)$$

where; $\alpha = \frac{2\pi}{5}$

The inverter with five legs has ability to produce the five-phase voltage, each leg has two switches operated in a complementary manner, resulting in 2^5 (32) internal states. The 0 and 31 states are zero vectors and the other thirty states are active vectors. These vectors are distributed in the main and auxiliary vector spaces in ten sectors, as shown in figure (5). It is clear that the active vectors are divided into three groups according to their amplitudes: small (S), medium (M), and large (L) space vectors, and their magnitudes are:

$$v_S = \frac{4}{5} \cos \frac{2\pi}{5} V_{dc} \tag{19}$$

$$v_M = \frac{2}{5} V_{dc} \tag{20}$$

$$v_L = \frac{4}{5} \cos \frac{\pi}{5} V_{dc} \tag{21}$$

It can be seen from figure (5) that the large active vectors of main frame ($d_1 - q_1$ plane) and small active vectors in auxiliary frame ($d_3 - q_3$ plane) are the same vectors, and the small active vectors in $d_1 - q_1$ plane and the large active vectors in $d_3 - q_3$ plane are the same too, while the medium active vectors are same in both planes.

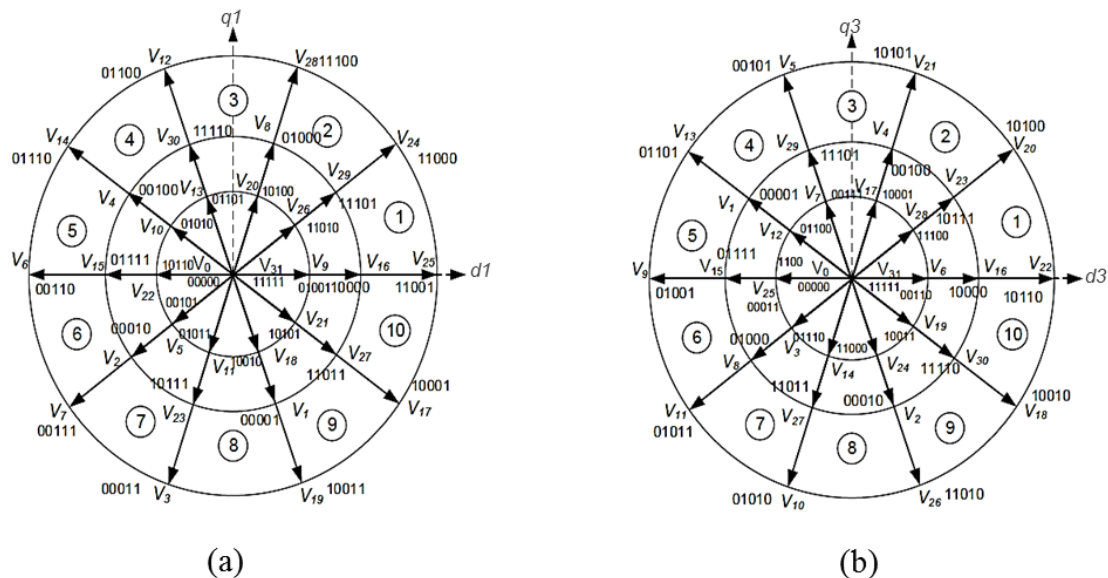


Figure (5): Space vector diagram of five-phase inverter (a) Main frame plane (b) Auxiliary frame plane

The reference output voltage in any sector can be generated by only two large active vectors in $d_1 - q_1$ plane which give small active vectors in $d_3 - q_3$ plane, thus low order voltage harmonics are generated, such as the 3rd and the 7th harmonics, due to these two large vectors, a sinusoidal output voltage cannot produce, also there is a reduction in reference voltage amplitude. In order to obtain the maximum reference output voltage as close as possible to the sinusoidal waveform, and due to that the number of active vectors applied for an odd phase number inverter should be less than

The number of inverter phases by one, the SVPWM scheme is based on the chosen of two large and two medium space vectors in the $d_1 - q_1$ plane, and the two small vectors are omitted which give large vectors in $d_3 - q_3$ plane [9].

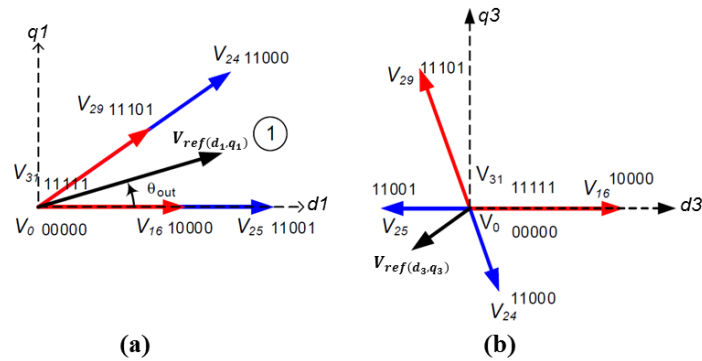


Figure (6): Chosen vectors for the reference output voltage in sector 1 in $d_1 - q_1$ plane
 (a) $d_1 - q_1$ plane (b) $d_3 - q_3$ plane

For the reference output voltage with θ_{out} between 0 and $\pi/5$, as example, it located in sector 1 in $d_1 - q_1$ plane, the active vectors that are used to generate this reference output voltage are V_{16} , V_{29} , V_{25} , and V_{24} , which form the reference voltages $V_{ref(d_1,q_1)}$ and $V_{ref(d_3,q_3)}$ in $d_1 - q_1$ and $d_3 - q_3$ planes, respectively, as shown in figure (6), with the following constrains:

$$V_{ref(d_1,q_1)} = d_{16}V_{16(d_1,q_1)} + d_{29}V_{29(d_1,q_1)} + d_{25}V_{25(d_1,q_1)} + d_{24}V_{24(d_1,q_1)} \quad (22)$$

$$V_{ref(d_3,q_3)} = d_{16}V_{16(d_3,q_3)} + d_{29}V_{29(d_3,q_3)} + d_{25}V_{25(d_3,q_3)} + d_{24}V_{24(d_3,q_3)} \quad (23)$$

where; d_{16} , d_{29} , d_{25} , and d_{24} are the duty cycles of chosen active vectors in sector 1. The duty cycles of the zero vectors are:

$$d_0 = d_{31} = \frac{1}{2}(1 - d_{16} - d_{29} - d_{25} - d_{24}) \quad (24)$$

Table (IV): The chosen active vectors for reference output voltage in d_1-q_1 plane

Sector	Chosen active vectors
1	$V_{16} - V_{29} - V_{25} - V_{24}$
2	$V_{29} - V_8 - V_{24} - V_{28}$
3	$V_8 - V_{30} - V_{28} - V_{12}$
4	$V_{30} - V_4 - V_{12} - V_{14}$
5	$V_4 - V_{15} - V_{14} - V_6$
6	$V_{15} - V_2 - V_6 - V_7$
7	$V_2 - V_{23} - V_7 - V_3$
8	$V_{23} - V_1 - V_3 - V_{19}$
9	$V_1 - V_{27} - V_{19} - V_{17}$
10	$V_{27} - V_{16} - V_{17} - V_{25}$

According to sector 1, the general form for $V_{ref(d_1,q_1)}$ and $V_{ref(d_3,q_3)}$ in any sector is:

$$\begin{bmatrix} V_{ref}(d_1) \\ V_{ref}(q_1) \\ V_{ref}(d_3) \\ V_{ref}(q_3) \end{bmatrix} = \begin{bmatrix} V_L & V_L \cos \frac{\pi}{5} & V_M & V_M \cos \frac{\pi}{5} \\ 0 & V_L \sin \frac{\pi}{5} & 0 & V_M \sin \frac{\pi}{5} \\ -V_S & V_S \cos \frac{2\pi}{5} & V_M & V_M \cos \frac{3\pi}{5} \\ 0 & -V_S \sin \frac{2\pi}{5} & 0 & V_M \sin \frac{3\pi}{5} \end{bmatrix} \begin{bmatrix} d_L \\ d_{Le\frac{\pi}{5}} \\ d_M \\ d_{Me\frac{\pi}{5}} \end{bmatrix} \quad (25)$$

where; d_L and d_M are the duty cycle of the large and medium vectors, respectively, which give the duty cycles of active vectors as:

$$\begin{bmatrix} d_L \\ d_{Le\frac{\pi}{5}} \\ d_M \\ d_{Me\frac{\pi}{5}} \end{bmatrix} = \begin{bmatrix} V_L & V_L \cos \frac{\pi}{5} & V_M & V_M \cos \frac{\pi}{5} \\ 0 & V_L \sin \frac{\pi}{5} & 0 & V_M \sin \frac{\pi}{5} \\ -V_S & V_S \cos \frac{2\pi}{5} & V_M & V_M \cos \frac{3\pi}{5} \\ 0 & -V_S \sin \frac{2\pi}{5} & 0 & V_M \sin \frac{3\pi}{5} \end{bmatrix}^{-1} \begin{bmatrix} V_{ref}(d_1) \\ V_{ref}(q_1) \\ V_{ref}(d_3) \\ V_{ref}(q_3) \end{bmatrix} \quad (26)$$

and duty cycles of zero vectors are shared equally as:

$$d_0 = d_{31} = \frac{1}{2} (1 - d_L - d_{Le\frac{\pi}{5}} - d_M - d_{Me\frac{\pi}{5}}) \quad (27)$$

In order to supply the load with sinusoidal voltages, the low-order harmonics need to be minimized, which mean the reference voltage in $d_3 - q_3$ plane regarded as zero [4], $V_{ref}(d_3, q_3) = 0$, and the reference output voltage mapped onto the reference voltage in $d_1 - q_1$ plane only.

Returning to sector 1, the duty cycle of two large active vectors are:

$$d_{25} = \frac{m_i}{5 \sin \frac{\pi}{5}} \left(\frac{\tau}{1+\tau^2} \right) \sin \left(\frac{\pi}{5} - \theta_{out} \right) \quad (28)$$

$$d_{24} = \frac{m_i}{5 \sin \frac{\pi}{5}} \left(\frac{\tau}{1+\tau^2} \right) \sin(\theta_{out}) \quad (29)$$

and the duty cycles of two medium active vectors are:

$$d_{16} = \frac{m_i}{5 \sin \frac{\pi}{5}} \left(\frac{1}{1+\tau^2} \right) \sin \left(\frac{\pi}{5} - \theta_{out} \right) \quad (30)$$

$$d_{29} = \frac{m_i}{5 \sin \frac{\pi}{5}} \left(\frac{1}{1+\tau^2} \right) \sin(\theta_{out}) \quad (31)$$

where; $\tau = 2 \cos \frac{\pi}{5}$, θ_{out} is the angle of the reference output voltage, m_i is modulation index of the inverter stage, it is defined as:

$$m_i = 2 \frac{V_{out}}{V_{dc}} \quad (32)$$

and the maximum value of m_i is:

$$m_{i(\max)} = \frac{1}{\cos\frac{\pi}{10}} \quad (33)$$

The voltage transfer ratio of the three to five-phase IMC is defined as:

$$q = \frac{V_{out}}{V_{in}} \quad (34)$$

From equations (11), (32), (33), and (34) the maximum voltage transfer ratio of the three to five-phase IMC is [4]:

$$q_{max} = \frac{3}{2} \frac{1}{2} \frac{1}{\cos\frac{\pi}{10}} = 0.7886 \quad (35)$$

2.3. Synchronization Between Rectifier and Inverter Stages

In one sampling period, there are two switching states in rectifier stage that produce two line-to-line voltages, which converted to the dc-link voltage. According to equations (10) and (11), the five-phase inverter fed by two positive line-to-line input voltages. Therefore, there are two groups of the switching states in the inverter stage. The switching states of the rectifier and inverter stages should be mixed to obtain balanced three phase input current and five-phase output voltage, and their duty cycles are obtained by cross product of the duty cycles of both stages, as shown in figure (7) for sector 1:

$$d_{25(ab)} = d_{25} d_x ; d_{25(ac)} = d_{25} d_y \quad (36)$$

$$d_{24(ab)} = d_{24} d_x ; d_{24(ac)} = d_{24} d_y \quad (37)$$

$$d_{16(ab)} = d_{16} d_x ; d_{16(ac)} = d_{16} d_y \quad (38)$$

$$d_{29(ab)} = d_{29} d_x ; d_{29(ac)} = d_{29} d_y \quad (39)$$

$$d_{0(ab)} = d_0 d_x ; d_{0(ac)} = d_0 d_y \quad (40)$$

$$d_{31(ab)} = d_{31} d_x ; d_{31(ac)} = d_{31} d_y \quad (41)$$

For zero dc-link current commutation in rectifier stage, as shown in figure (7), all currents are zero in rectifier stage, due to zero vectors applied in inverter stage during the commutation. The complex multi-step commutation processes can be avoided, and the switching losses of the rectifier stage can be reduced due to zero dc-link current commutation [4].

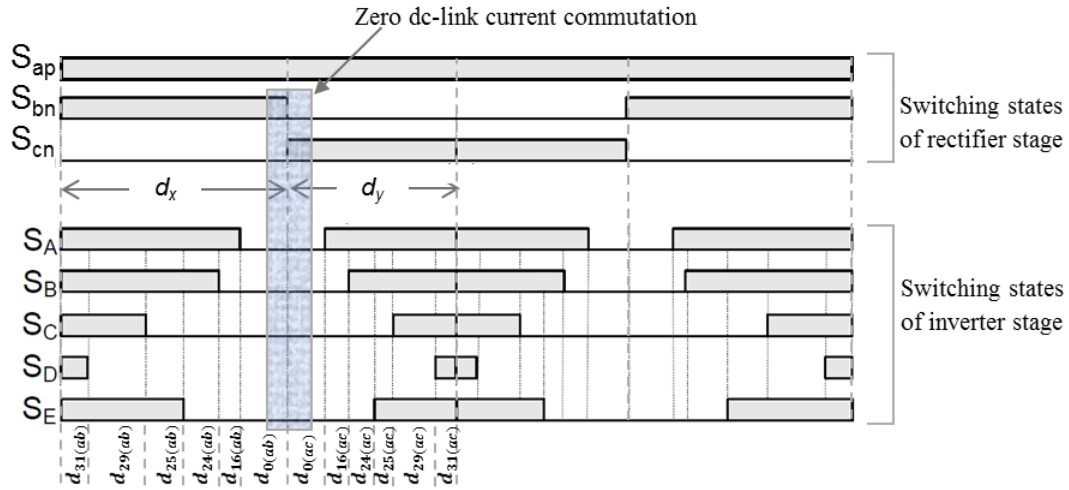


Figure (7): switching states of rectifier and inverter stages

3. The Carrier Based Pulse Width Modulation (CBPWM)

In space vector pulse width modulation (SVPWM) there are two modulations for rectifier and inverter stages, each SVPWM needs a complex process as a selection of effective vectors and determine their duty cycles by calculating various equations independently for both stages, the switching states of both stages are arranged to achieve zero dc-link current commutation and balanced output voltages. Therefore, the SVPWM needs many calculations and tables to complete the process. In order to avoid the complexity, the CBPWM is developed to generate gating signals of switching easily for rectifier and inverter stages.

In the CBPWM method, the PWM signals are generated according the comparison between the modulation signals and high-frequency carrier signal. The calculation of modulation signals based on the duty cycles of the rectifier stage, the reference output voltage and the average dc-link voltage [1],[4].

The carrier signal that used to generate the PWM signals is symmetrical triangular signal in rectifier stage and unsymmetrical triangular signal in inverter stage, a variable-slope carrier modulation scheme controls the inverter stage. The carrier signal rising and falling edges slopes are varying in every sampling period. The duty cycles of the rectifier switches and variation in dc-link voltage are based on the rising and falling intervals of the carrier signal [2],[4]. In this paper a fixed slope carrier signal is used for all switches in both stages instead of variable slope carrier signal to simplify the implementation of the CBPWM process, which described by:

$$v_t = \left(\frac{4}{T_s} t - 1\right) V_{in} ; \quad 0 \leq t \leq T_s \tag{42}$$

where; V_{in} is the amplitude of input phase voltage, v_t is the instantaneous value of carrier signal, T_s is the sampling time.

3.1. Rectifier Stage Control

The timing and sequence of modulated switches of the reference input current vector in sector 1, as well as the carrier and modulation signals required to generate the PWM of the rectifier stage are shown in figure (8).

For half one sampling period, T_n the duration of gating pulse of switch S_{bn} is:

$$T_n = d_x \frac{T_s}{2} \tag{43}$$

From equations (42) and (43), the modulation signal of rectifier stage is obtained by:

$$V_n = (2d_x - 1) V_{in} \tag{44}$$

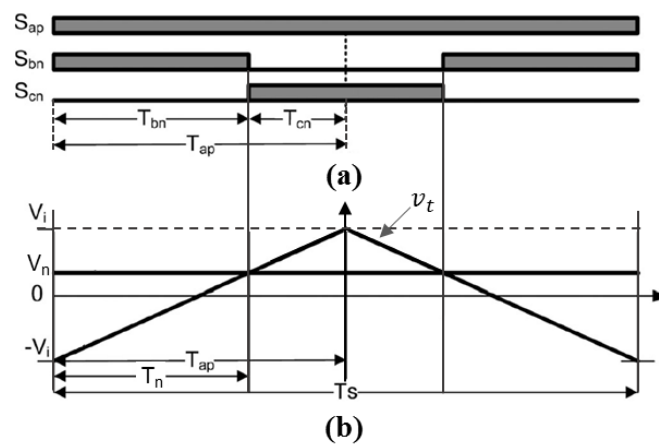


Figure (8): Generation of PWM for rectifier switch
 (a) Switching states of rectifier stage (b) Carrier and modulation signals

The gating pulse of switch S_{bn} (PWM0) is obtained by intersection the modulation signal, V_n , with the carrier signal, v_t . The gate pulse of switch S_{cn} (PWM1) is complementary to that of S_{bn} . And all the other switches, S_{an} , S_{bp} , and S_{cp} are in off-state. Table (V) shows the gating pulses of switches for six sectors.

Table (V): The switching states of rectifier stage

Sector	S_{ap}	S_{an}	S_{bp}	S_{bn}	S_{cp}	S_{cn}
1	1	0	0	PWM0	0	PWM1
2	PWM0	0	PWM1	0	0	1
3	0	PWM1	1	0	0	PWM0
4	0	1	PWM0	0	PWM1	0
5	0	PWM0	0	PWM1	1	0
6	PWM1	0	0	1	PWM0	0

3.2. Inverter Stage Control

In the traditional five-phase inverter fed by constant dc voltage, only five modulation signals are used to compare with the carrier signal in one sampling period. For IMC the dc-link voltage has two values depending on the voltages of input source, therefore, the

switching pattern of the inverter stage consists of two parts with different values, and the switching frequency of the inverter is twice of the switching frequency of the rectifier. There are two modulation signals for the inverter stage are obtained from the duty cycles of the rectifier stage d_x and d_y , these signals are compared with the carrier signal to generate two pulses, by applied the XNOR function, the gate signal of the upper switch is obtained for each phase of the inverter, and the gate signal of the lower switch is the complement of that the upper [1]. The using of XNOR function is to insert zero state in the switching period to make the CBPWM is the same as the SVPWM and get the same properties, the zero state is necessary to solve the commutation problem. In sector 1 as example, the two modulation signals V_{A1} and V_{A2} are determined according to v_{ab} and v_{ac} , respectively, these signals are compared with the carrier signal v_t to generate two pulses S_{A1} and S_{A2} , then the gate signal of switch S_A is determined by:

$$S_A = S_{A1} \cdot S_{A2} + \overline{S_{A1}} \cdot \overline{S_{A2}} \tag{45}$$

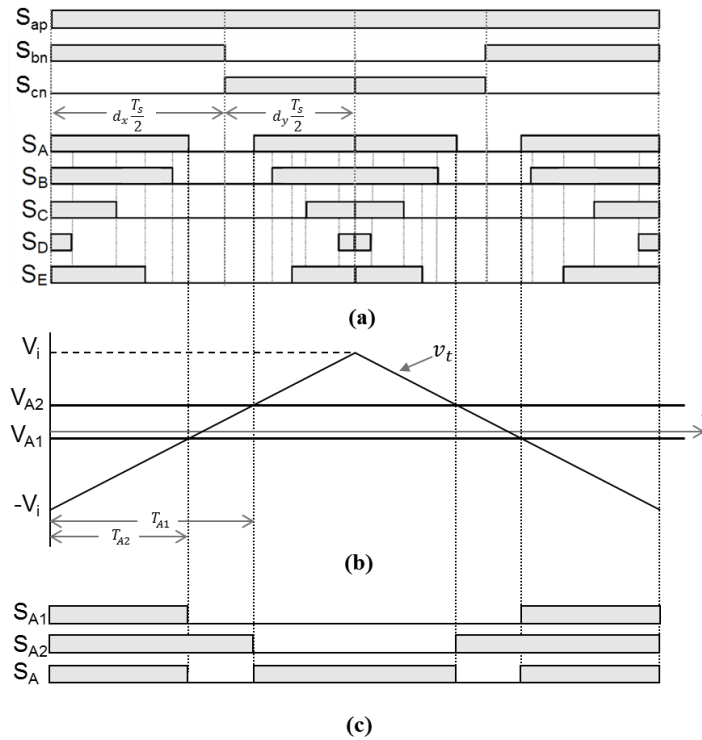


Figure (9): Generation of PWM for inverter switch (a) Switching states of IMC stages (b) Carrier and modulation signals (c) Gate signal of switch A

Figure (9) shows the generation of the gate signal of upper switch of phase-A, the durations T_{A1} and T_{A2} can be written as follows:

$$T_{A1} = (d_{31(ab)} + d_{29(ab)} + d_{25(ab)} + d_{24(ab)} + d_{16(ab)}) \frac{T_s}{2} = (d_x - d_{0(ab)}) \frac{T_s}{2} \tag{46}$$

$$T_{A2} = (d_{31(ab)} + d_{29(ab)} + d_{25(ab)} + d_{24(ab)} + d_{16(ab)} + d_{0(ab)} + d_{0(ac)}) \frac{T_s}{2} = (d_x + d_{0(ac)}) \frac{T_s}{2} \tag{47}$$

By substituting the equations above into equation (42), the two modulation signals V_{A1} and V_{A1} are:

$$v_{A1} = \left(-2d_y \frac{v_A + v_{offset}}{\bar{V}_{dc}} + d_x\right) V_{in} \tag{48}$$

$$v_{A2} = \left(2d_x \frac{v_A + v_{offset}}{\bar{V}_{dc}} - d_y\right) V_{in} \tag{49}$$

where; v_{offset} is the offset voltage:

$$v_{offset} = -\frac{1}{2}(v_A + v_D) \tag{50}$$

The above three equations (48-50) are obtained for reference output located in sector 1. These equations can be generalized for a reference output voltage in any sector to obtain the modulation signals to any switch S_X (X: A, B, C, D, E) in the inverter stage, as follows:

$$v_{X1} = \left(-2d_y \frac{v_X + v_{offset}}{\bar{V}_{dc}} + d_x\right) V_{in} \tag{51}$$

$$v_{X2} = \left(2d_x \frac{v_X + v_{offset}}{\bar{V}_{dc}} - d_y\right) V_{in} \tag{52}$$

$$v_{offset} = -\frac{1}{2}(v_{max} + v_{min}) \tag{53}$$

where; v_X is the fundamental output phase voltage, which given in (12-16), $v_{max} : \max(v_A, v_B, v_C, v_D, v_E)$, $v_{min} : \min(v_A, v_B, v_C, v_D, v_E)$.

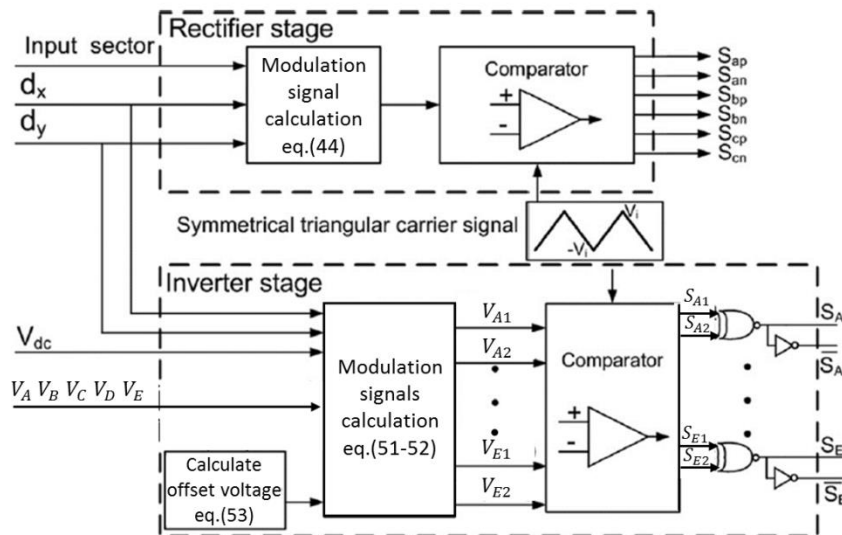


Figure (10): Block diagram of the CBPWM method.

Figure (10) shows the block diagram of the CBPWM for the two stages of the IMC. The required gate signals of the rectifier stage and the inverter stage can be generated

easily without complex calculations. The performance of this modulation method is the same of SVPWM method because it is based on the mathematical analysis of SVPWM, which is clear in the relationship between the offset voltage in CBPWM and distribution of zero vectors in SVPWM [2],[1],[4].

4. Simulation Results

The simulink block diagram of the V/f speed control system, IMC system, and CBPWM system are shown in figure (11). The signal generator in figure (11-a) is used to generate three signals: carrier signal, input signal information, and the reference output voltages. The aforementioned signals are used to provide the IMC with the required information to convert three-phase voltages to five-phase voltages and fed the load.

Figure (11-b) shows the signals of the signal generator block, the *Carrier Signal* port contains the symmetrical triangular carrier signal, the *input signal information* port contains the three-phase input voltages in addition to the magnitude and ω_{int} of phase *a*. The *reference output signal* port contains the five-phase output voltages.

The IMC construction is shown in figure (11-c) where the rectifier and inverter get their control signal from the CBPWM block, the input filter is used to smooth the input currents and enhance the input power factor. The construction of the CBPWM block is shown in figure (11-d) which represents equations that are required to generate the control signals. The parameters of the simulation model are shown in table (VI).

Table (VI): Parameters of simulation model [10]

Parameters	Data
Three-phase input supply	peak phase voltage 270 V, f=60 Hz
Input filter	$C_f=20\mu\text{F}$, $L_f=1\text{mH}$, $R_f=1\Omega$
Parameters of motor	$R_s=2.07\Omega$, $L_a=0.01\text{H}$, Pole pairs=2, flux linkage= 0.75 V.s $J=0.0015\text{ kg.m}^2$, $B=0.001\text{ N.m.s}$ Full load=4N.m
Five-phase output signal	V/f ratio= 20/5, f=50 Hz
Carrier signal	f=5kHz

Figure (12) shows the simulation results at full load of 4 N.m with constant speed at 1500 r.p.m. In figure (12-a) the speed response of the five-phase PMSM reaches the steady state after 0.1 second and shows oscillation with overshoot of 1.33%, the starting problem is solved by increasing the voltage and frequency as ramp signals with slope of 15000 r.p.m/second.

The actual torque and the reference torque (4 N.m) are shown in figure (12-b), the actual torque is increased gradually to oscillate between 6 and 8 N.m due to the change in speed with respect to time ($\frac{d\omega}{dt}$), then decreased to oscillate about 4 N.m as speed reaches steady state.

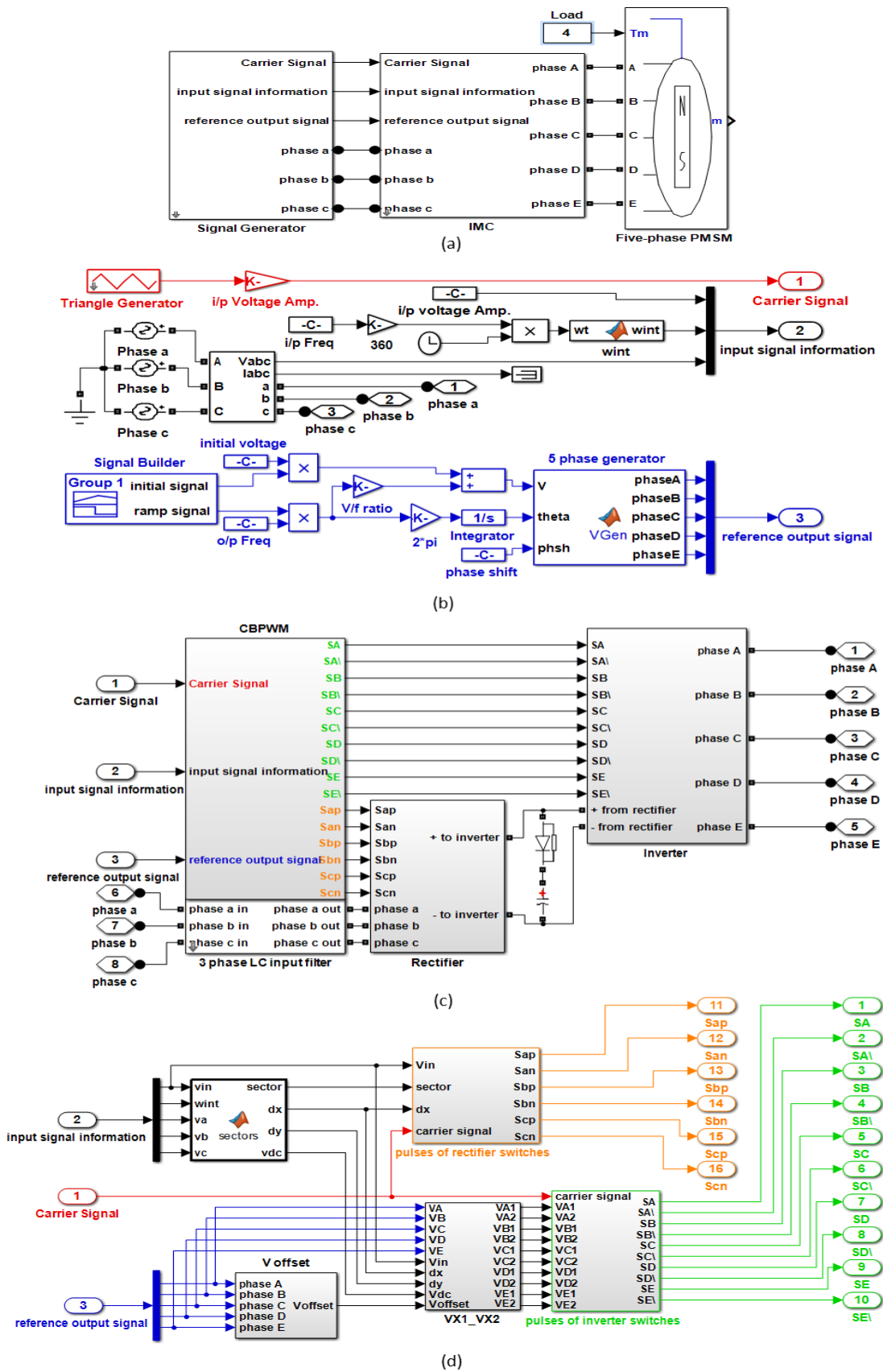


Figure (11): The simulink block diagram systems (a) V/f speed control system (b) Signal generator (c) IMC system (d) CBPWM system

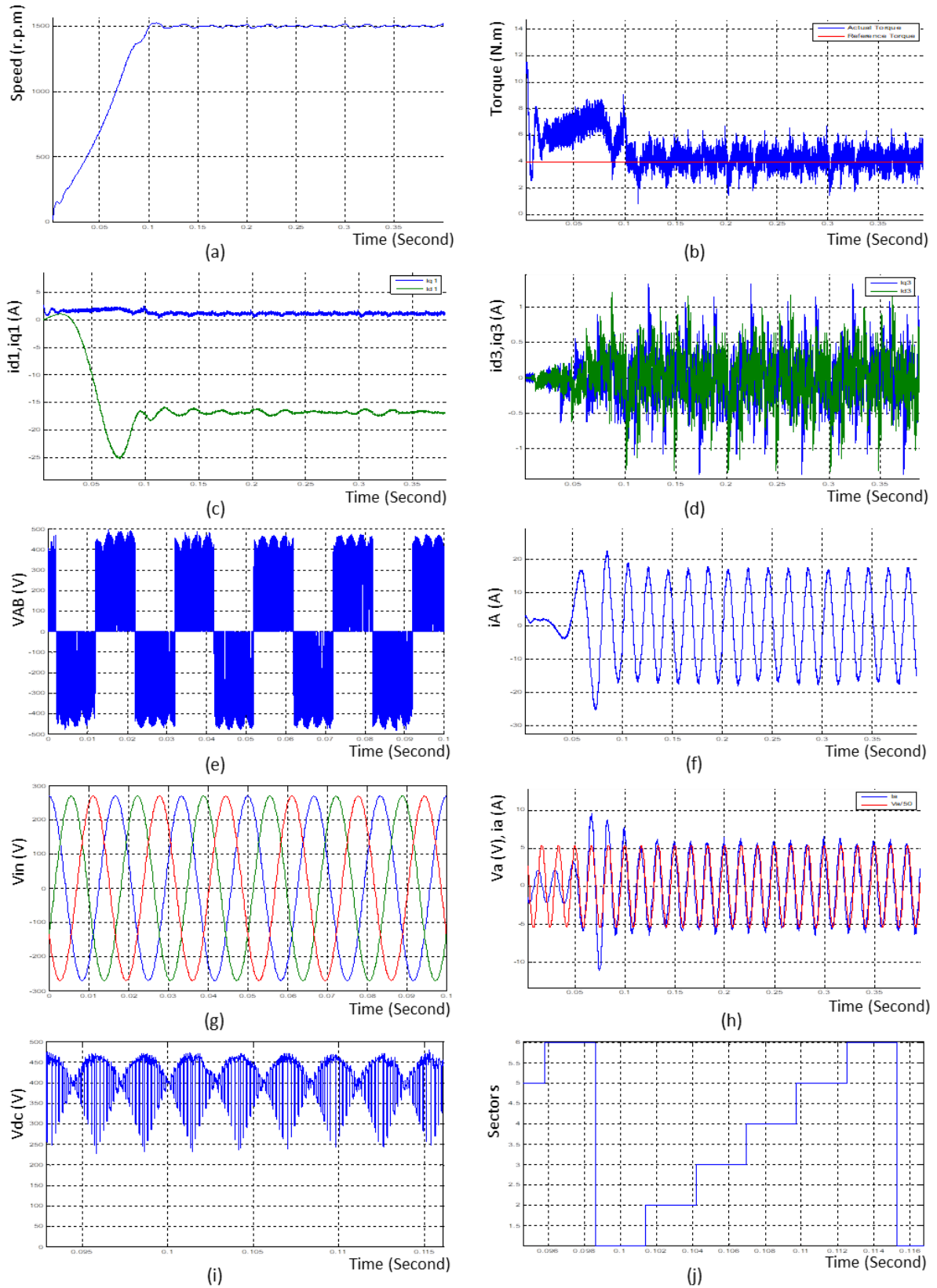


Figure (12): Simulation results with constant load and speed (a) Speed response (b) Torque response (c) id1 and iq1 (d) id3 and iq3 (e) Output voltage (f) Output current (g) Input voltage (h) Input voltage and current (i) dc-link voltage (j) Sectors

Figure (12-c) shows the stator currents (i_{d1} and i_{q1}) which are reaches -17 A and 1.1 A at steady state, respectively. These currents represent the flux and torque components respectively, while figure (12-d) shows the i_{d3} and i_{q3} currents, which are oscillated about zero with a clear effect of the third and other harmonics as shown in table (III).

The five-phase line-to-line output voltage (V_{AB}) with peak value 470 V and frequency 50 Hz is shown in figure (12-e). The sinusoidal output current of phase A (I_A) is shown in figure (12-f), it seems sinusoidal waveform due to neglect the i_{d3} and i_{q3} currents in the analysis of the inverter stage control, the output current reaches steady state after 0.1 second with peak value 17.5 A and frequency 50 Hz.

The input three-phase voltages and the input voltage and current of phase a; V_a and I_a , with peak values 270 V, 6 A, and frequency 60 Hz are shown in Figure (12-g) and Figure (12-h), respectively, it is clear from the figures that there is approximately 3° phase shift angle between the input voltage and current, V_a and I_a , due to the good adjustment of LC input filter parameters. Figure (12-i) shows the dc-link voltage with average value 400 V and its maximum and minimum values as 485 V and 220 V, respectively. In the meanwhile, the sectors corresponding to the dc-link voltage are shown in figure (12-j).

Figure (13) shows the simulation results with increasing load at time 0.3 second from 4 N.m to 6 N.m then decreasing load to 3 N.m at 0.65 second as shown in figure (13-b).

At the instant of increasing and decreasing the torque, the speed is little decreased and increased oscillatory with downshoot 2.5% and overshoot 3%, respectively. After that, the speed is stabilized at the synchronous speed as shown in figure (13-a).

The same effect occurs to the i_{d1} and i_{q1} , where they are increased from -17 A to -14.5 A and from 1.1 A to 1.7 A, respectively, then i_{q1} decreased to 1 A, due to increasing and decreasing the required torque. While i_{d3} and i_{q3} are not effected due to neglect them in PWM processing as shown in figures (13-c) and (13-d), respectively.

The output current is decreased from 17.5 A to 15.5 A while input current increased from 6 A to 6.5 A as increasing in load. After that, the output current is decreased to 13.5 A then reaches the steady state at 15.5 A. The input current is decreased to 4.5 A when the load is decreased as shown in figures (13-e) and (13-f).

Figure (14) shows the simulation results with decreasing the speed at time 0.35 second from 1500 r.p.m to 750 r.p.m as ramp function with slope of -15000 r.p.m/second and shows oscillation with downshoot of 4.7% then increasing to 1000 r.p.m at time 0.7 second as ramp function with slope of 5000 r.p.m/second and shows oscillation with overshoot of 3.4% as shown in figure (14-a).

The torque at 0.35 second is decreased from 4 N.m to 1 N.m then reaches steady state at 4 N.m after falling time of 0.05 second due to the change in speed with respect to time ($\frac{d\omega}{dt}$) as speed decreasing, then it is increased from 4 N.m to 6 N.m at 0.7 second then reaches steady state at 4 N.m after rising time of 0.05 second as speed increasing as shown in figure (14-b).

The same decrement and increment of the torque are occurred to the i_{q1} , which decreased from 1.1 A to 0.5 A at 0.35 second then reaches steady state at 1.1 A, and increased from 1.1 A to 1.3 A at 0.7 second then reaches steady state at 1.1 A too.

The i_{d1} is changed as speed and decreased from -17 A to -12 A then stabilized at -19 A and increased to -25 A then stabilized at -20.5 A as shown in figure (14-c). The changing in the speed is occurred due to changing in output frequency which is affected the harmonics as shown in figure (14-d).

The output current of phase a is changed in its amplitude and frequency due to the change in the speed, where it is decreased from 17.5 A with frequency 50 Hz to 13 A with frequency 25 Hz at speed 750 r.p.m with decreasing in the input current magnitude only to be 3 A, then they stabilized at 19 A for output current and 6 A for input current.

At speed 1000 r.p.m, the currents are increased to 25 A with frequency 33.333 Hz for output current and 10 A for input current, then they stabilized at 21 A for output current and 7 A for input current as shown in figures (14-e) and (14-f).

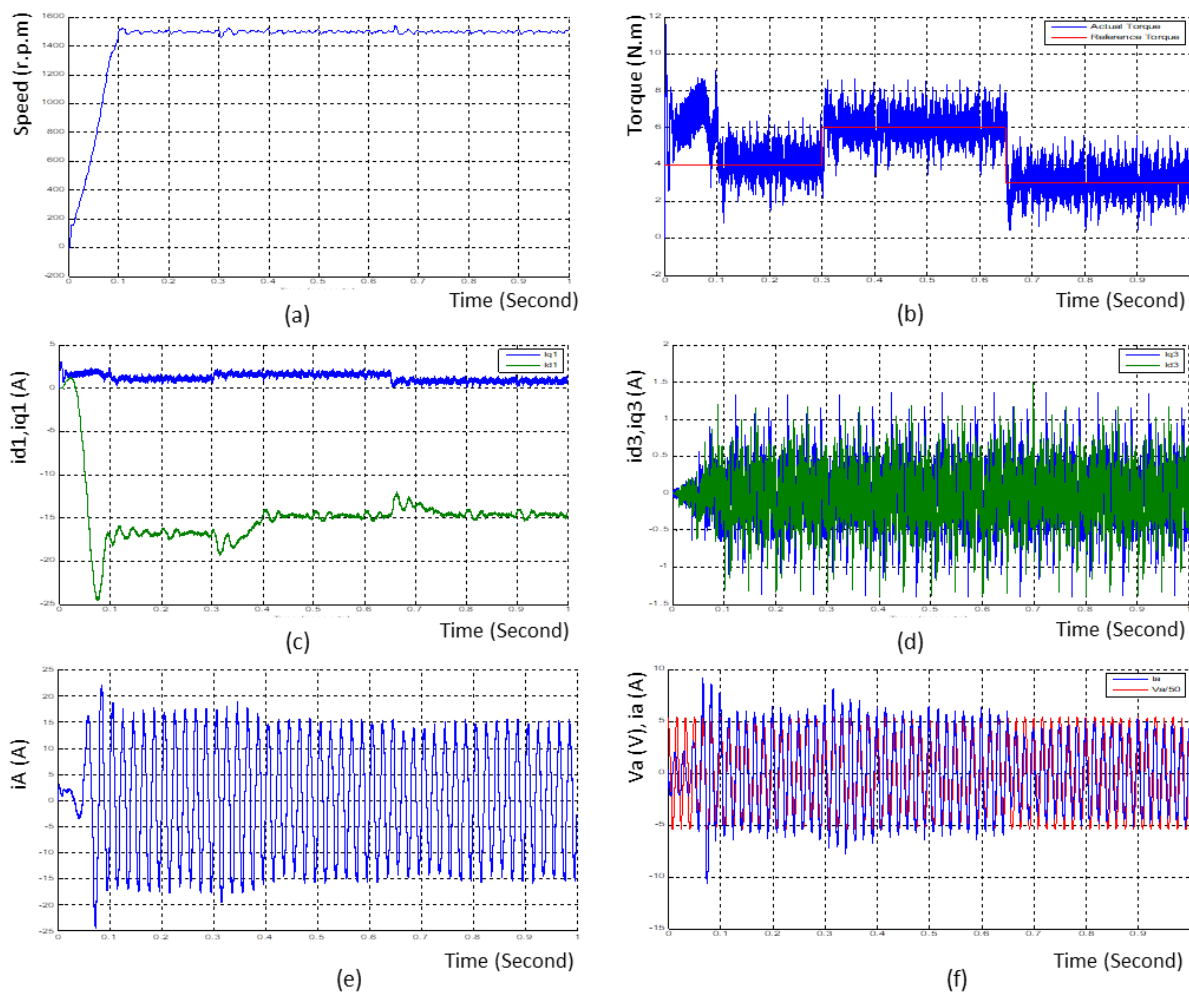


Figure (13): Simulation results with variable load (a) Speed response (b) Torque response (c) i_{d1} and i_{q1} (d) i_{d3} and i_{q3} (e) Output current (f) Input voltage and current

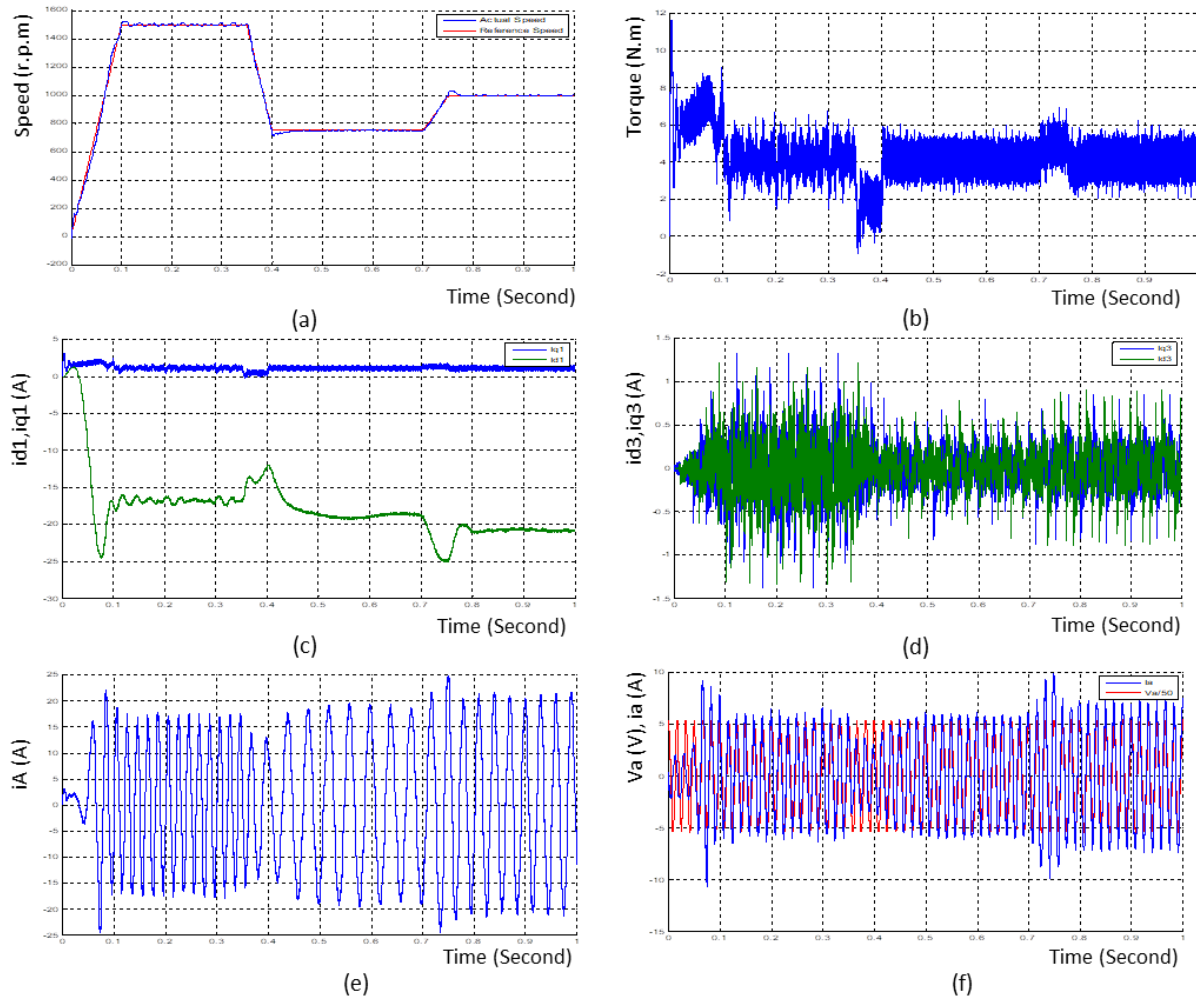


Figure (14): Simulation results with variable speed (a) Speed response (b) Torque response (c) i_{d1} and i_{q1} (d) i_{d3} and i_{q3} (e) Output current (f) Input voltage and current

The CBPWM method is not used to control the IMC switches with five-phase PMSM up to this time, it is only used for RL-load. Therefore no results of V/f speed control of five-phase PMSM fed by IMC with CBPWM are found in literature. For comparison a vector control of five-phase PMSM drive results [13] are used.

The vector control of PMSM drive system is tested under fixed speed of 100 rad/s with variable load as shown in figure (15). The speed response reaches 100 rad/s after 0.2 second with torque increased to 6 N.m then stabilized at no load, the load is changed from 0 to 4 N.m at 0.3 second with downshoot in speed of 10%, after that the load is decreased from 4N.m to 3 N.m at 0.7 second with overshoot in speed of 4%.

The q-current shows the same behavior of torque, where it is increased to 7 A at starting then stabilized at zero for no load, with load increasing to 4N.m, the q-current increased to 6 A then stabilized at 5 A, and decreased to 3.5 A as load decreased to 3 N.m. While d-current keeps constant as speed is fixed.

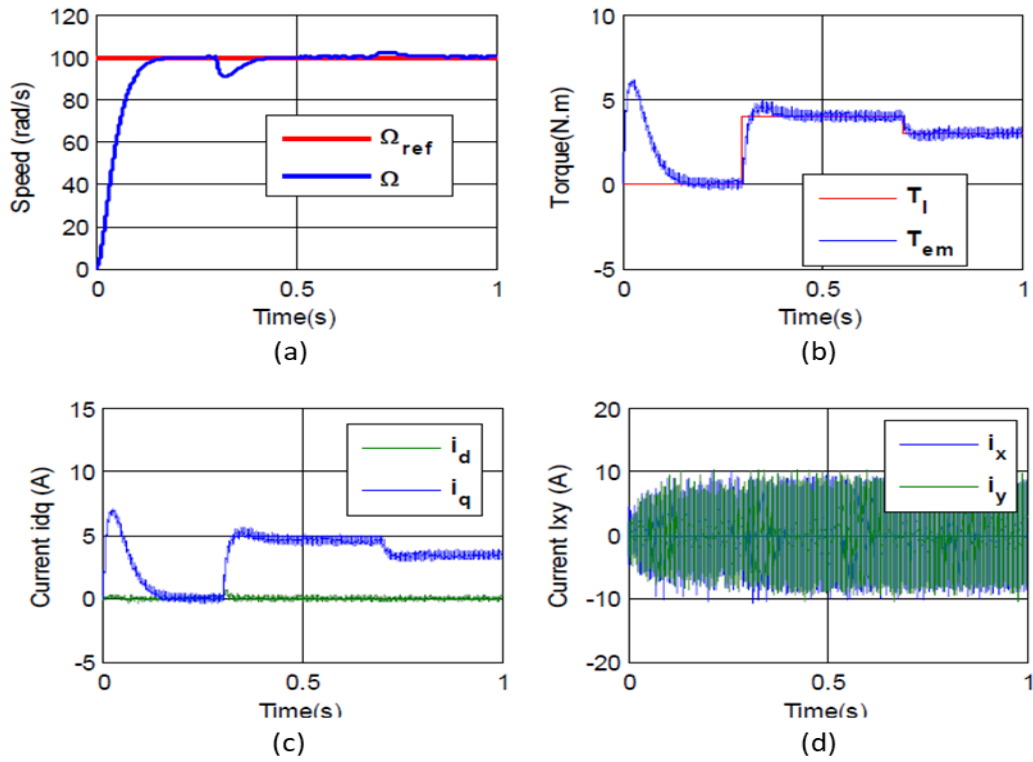


Figure (15): Results of vector control PMSM drive system with variable load (a) Speed response (b) Torque response (c) i_d and i_q (d) i_x and i_y [13]

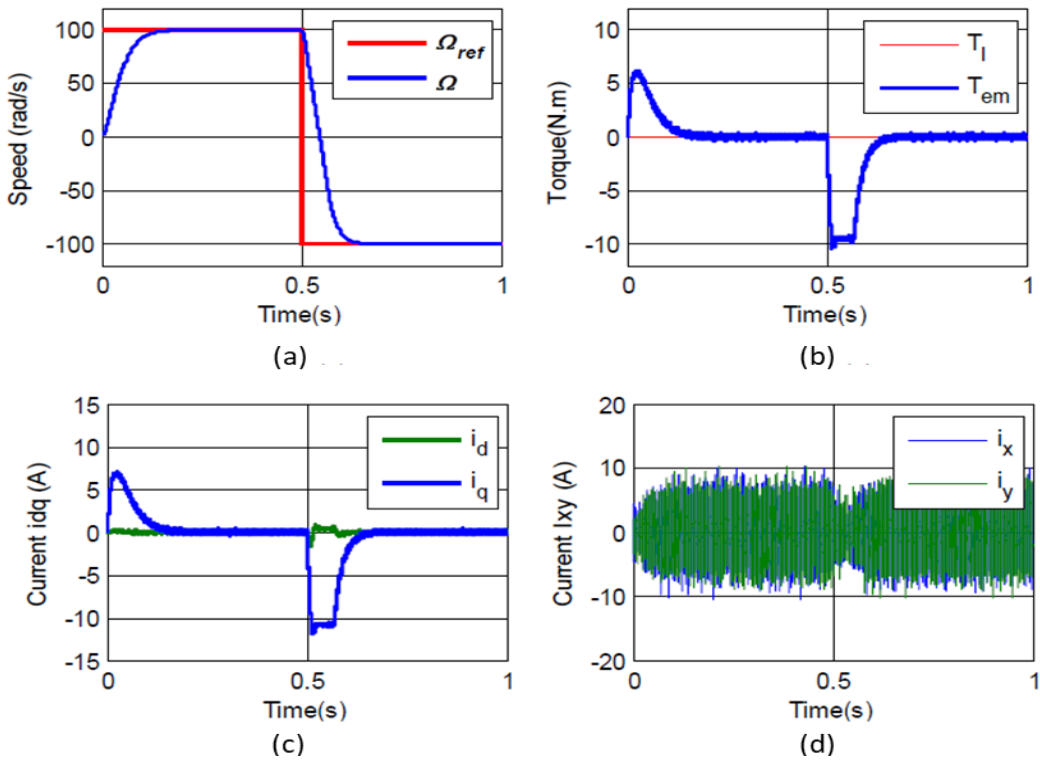


Figure (16): Results of vector control PMSM drive system with variable speed (a) Speed response (b) Torque response (c) i_d and i_q (d) i_x and i_y [13]

The vector control of PMSM drive system is tested again under no load with variable speed as shown in figure (16). The speed is changed from 100 rad/s to -100 rad/s with load decreased to -10.5 N.m then stabilized at no load after settling time of 0.2 second.

The q-current also decreased to -11 A then stabilized at zero just like the torque behavior, while d-current shows disturbance between -2 and 1 A till the speed reaches -100 rad/s.

5. Conclusions

In this paper, the IMC is used to feed the five-phase PMSM from grid directly, with applying the V/f control method to control the speed of motor, the following conclusions are outcome:

- The IMC provides sinusoidal output current from a sinusoidal input current with approximately unity input power factor.
- The CBPWM method which based on the SVM analysis is used instead of the SVPWM to control the two stages of the IMC and coupled them physically with a symmetrical triangular carrier signal.
- By adjustment the parameters of the input filter, the input current gives approximately a unity power factor for all cases (phase shift between input current and voltage is approximately 3°).
- The output current has a sinusoidal waveform shape due to neglect the d_3 - q_3 currents.
- The system is remained stable with variable load and speed with speed overshoot of (1.33%-3.4%).
- The i_{d1} and i_{q1} show overshoot with variable load and speed, this is due to the non-linear dynamic characteristics of PMSM, and also the V/f approach is an open loop type (there is no control loops for i_{d1} and i_{q1}).
- From the comparison with the vector controlled PMSM drive system results, the proposed V/f PMSM drive system is simple to implement and shows better speed response with overshoot less by three times.

6. References

1. T. D. Nguyen and H. H. Lee. (2014). "Dual Three-Phase Indirect Matrix Converter With Carrier-Based PWM Method". IEEE Transactions on Power Electronics, Volume: 29, Issue: 2, pp. 569-581.
2. T. D. Nguyen and H. H. Lee. (2012). "Generalized Carrier-based PWM Method for Indirect Matrix Converters". 3rd IEEE International Conference on Sustainable Energy Technologies (ICSET), Nepal, pp. 223-228.
3. Q. H. Tran, N. V. Nguyen, and H. H. Lee. (2014). "A Carrier-based Modulation Method to Reduce Switching Losses for Indirect Matrix Converters". IECON 40th Annual Conference of the IEEE Industrial Electronics Society, p.p 4828-4833.
4. T. D. Nguyen and H. H. Lee. (2016). "Development of a Three-to-Five-Phase Indirect Matrix Converter with Carrier-Based PWM Based on Space Vector

- Modulation Analysis*". IEEE Transactions on Industrial Electronics, Vol. 63, No. 1, pp 13-24.
5. A. Dieng, M. F. Benkhoris, A. B. Mboup, M. A. Ahmed, J. C. L. Clairel. (2016). "Analysis of Five-Phase Permanent Magnet Synchronous Motor". Rev. Roum. Sci. Techn.– Électrotechn. et Énerg. Vol. 61, No. 2, pp. 116–120.
 6. L. Parsa. (2005). "Performance Improvement of Permanent Magnet Ac Motors". Ph.D. Thesis, Department of Electrical Engineering, Texas A&M University, College Station, Texas.
 7. Behera PK, Behera MK, Sahoo AK. (2014). "Speed Control of Induction Motor using Scalar Control". Proc. Int. conf. on Emergent Trends in Computing and Communication (ETCC-2014), pp. 37-39.
 8. X. Liu, F. Blaabjerg, P. C. Loh, and P. Wang. (2012). "Carrier-based Modulation Strategy and Its Implementation for Indirect Matrix Converter under Unbalanced Grid Voltage Conditions". 15th International Power Electronics and Motion Control Conference (EPE/PEMC), Europe, Novi Sad, Serbia, pp. LS6a.2-1-LS6a.2-7.
 9. A. Iqbal and E. Levi. (2005). "Space Vector Modulation Schemes for a Five-Phase Voltage Source Inverter". European Conference on Power Electronics and Applications, pp. 12 pp. - P.12.
 10. M. Kiuchi, T. Ohnishi, H. Hagiwara, Y. Yasuda. (2010). "V/f control of permanent magnet synchronous motors suitable for home appliances by DC-link peak current control method". The 2010 International Power Electronics Conference (ECCE ASIA), p-p. 567 – 573.
 11. P. D. C. Perera, F. Blaabjerg, J. K. Pedersen, P. Thogersen. (2003). "A sensorless, stable V/f control method for permanent-magnet synchronous motor drives". IEEE Transactions on Industry Applications, Vol. 39, No. 3, p-p. 783 – 791.
 12. P. A. Dahono, Deni C. P. Akbarifutra, A. Rizqiwawan. (2010). "Input ripple analysis of five-phase pulse width modulated inverters". IET Power Electronics, Vol. 3, No. 3, p-p. 716 – 723.
 13. T. Kamel, D. Abdelkader, B. Said. (2015). "Vector control of five-phase permanent magnet synchronous motor drive". 2015 4th International Conference on Electrical Engineering (ICEE), p-p. 1-4.

Appendix – A

The model of five-phase PMSM could be summarized as [6]:

$$v_{d1} = R_s i_{d1} + \frac{d\lambda_{d1}}{dt} - \omega \lambda_{q1} \quad (\text{A-1})$$

$$v_{q1} = R_s i_{q1} + \frac{d\lambda_{q1}}{dt} + \omega \lambda_{d1} \quad (\text{A-2})$$

$$v_{d3} = R_s i_{d3} + \frac{d\lambda_{d3}}{dt} - 3\omega \lambda_{d3} \quad (\text{A-3})$$

$$v_{q3} = R_s i_{q3} + \frac{d\lambda_{q3}}{dt} + 3\omega \lambda_{d3} \quad (\text{A-4})$$

$$\lambda_{d1} = (L_l + \frac{5}{2}L_{m1})i_{d1} + \lambda_{m1} \quad (\text{A-5})$$

$$\lambda_{q1} = (L_l + \frac{5}{2}L_{m1})i_{q1} \quad (\text{A-6})$$

$$\lambda_{d3} = (L_l + \frac{5}{2}L_{m3})i_{d3} + \lambda_{m3} \quad (\text{A-7})$$

$$\lambda_{q3} = (L_l + \frac{5}{2}L_{m3})i_{q3} \quad (\text{A-8})$$

$$T_e = \frac{5p}{2}(\lambda_{d1}i_{q1} - \lambda_{q1}i_{d1} + 3\lambda_{d3}i_{q3} - 3\lambda_{q3}i_{d3}) \quad (\text{A-9})$$

Where:

$v_{d1}, v_{q1}, v_{d3}, v_{q3}$: the stator voltages in $d_1, q_1, d_3,$ and q_3 axis.

$i_{d1}, i_{q1}, i_{d3}, i_{q3}$: the stator currents in $d_1, q_1, d_3,$ and q_3 axis.

$\lambda_{d1}, \lambda_{q1}, \lambda_{d3}, \lambda_{q3}$: the stator fluxes in $d_1, q_1, d_3,$ and q_3 axis.

$\lambda_{m1}, \lambda_{m3}$: the amplitude of fundamental and third harmonics components of permanent magnet flux linkages.

R_s : stator resistance.

Figure (A-1) shows the $d_1, q_1, d_3,$ and q_3 space of five-phase PMSM where the phase shift between two phases is 72° .

The Mechanical motion equation is given by:

$$T_e = T_L + J \frac{d\omega}{dt} + B\omega \quad (\text{A-10})$$

where T_e and T_L are the electromagnetic torque (developed torque) and load torque, J and B are the inertia moment and friction factor, and ω is the mechanical speed. The value of $J \frac{d\omega}{dt}$ is zero when the speed at steady state.

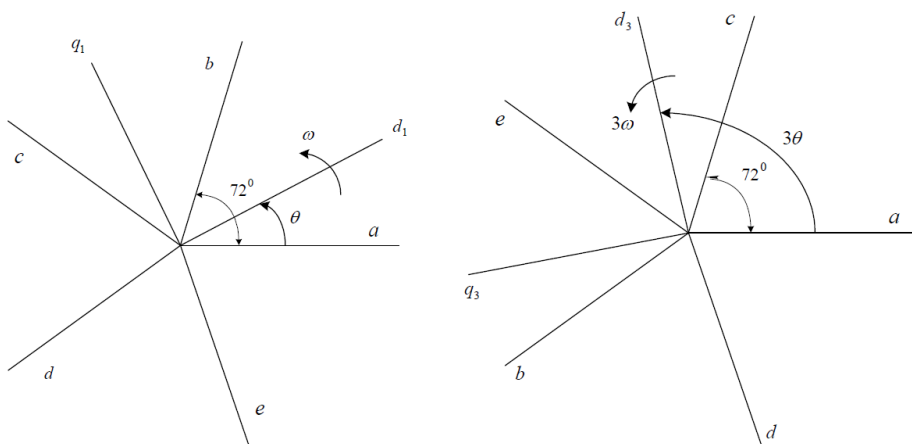


Figure (A-1): the $d_1, q_1, d_3,$ and q_3 space